UDC 528.87+528.855

FOREST ANISOTROPY ASSESSMENT BY MEANS OF SPATIAL VARIATIONS ANALYSIS OF POLSAR BACKSCATTERING

A. V. Dmitriev, T. N. Chimitdorzhiev, P. N. Dagurov

Institute of Physical Material Science, Russian Academy of Sciences, Siberian Branch
Sakh'yanova str., 6, Ulan-Ude, Republic of Buryatia, 670047 Russian Federation

E-mail: scidir@ipms.bscnet.ru

Received 01.12.2016

The possibility to synthesize polarization response from earth covers at any desired combination of transmit and receive antenna polarizations is the significant advantage of polarimetric radar. It permits better identification of dominant scattering mechanisms especially when analyzing polarization signatures. These signatures depict more details of physical information from target backscattering in various polarization bases. However, polarization signatures cannot reveal spatial variations of the radar backscattering caused by volume heterogeneity of a target. This paper proposes a new approach for estimating volume target heterogeneity from polarimetric synthetic aperture radar (PolSAR) images. The approach is based on the analysis of a novel type of polarization signature, which we call fractal polarization signature (FPS). This signature is a result of polarization synthesis of initial fully polarimetric data and subsequent fractal analysis of synthesized images. It is displayed as a 3D plot and can be produced for each point in an image. It is shown that FPS describes backscattering variations or image roughness at different states of polarization. Fully polarimetric data of SIR-C and ALOS PALSAR at ascending/descending orbits were used for testing the proposed approach. The azimuthal dependence of the radar backscattering variations is discovered when analyzing backscattering from a pine forest. It correlates with the results of a field survey of trees branch distribution.

Keywords: *radar imaging, polarization signature, fractal dimension, spatial variations.*

How to cite: *Dmitriev A. V., Chimitdorzhiev T. N., Dagurov P. N.* Forest anisotropy assessment by means of spatial variations analysis of PolSAR backscattering // *Sibirskij Lesnoj Zurnal* (Siberian Journal of Forest Science). 2017. N. 3: 19–27 (in English with Russian abstract).

DOI: 10.15372/SJFS20170302

INTRODUCTION

Monitoring of the boreal forest including Siberian taiga is an important for the assessment of global natural processes. Currently the most promising research tool for the remote sensing of forests are synthetic aperture radars (SAR). They allow us to evaluate forest stand and its biomass on the basis of empirical and theoretical models as shown in review (Sinha et al., 2015). Existing forest models implies a symmetric azimuthal distribution of the trees branches relative to the trunks. However, the coniferous forests have a greater number of branches from the more illuminated south side as shown by the results of field studies (Xiao et al., 2015). Therefore, it is necessary to develop such methods of data processing that will allow us to estimate azimuthal anisotropy of radar targets. This will allow to adjust the existing forest models and perform a more accurate assessment of its structure for monitoring purposes.

Specific features of electromagnetic waves interaction with complex structures that induce multiple scattering or have spatial anisotropy can be found by means of polarization measurements. Such measurements are ensured by a polarimetric SAR radiating linearly polarized waves with vertical (*V*) and horizontal (*H*) polarizations and receiving the reflected signal at matched (*VV* and *HH* signals) and orthogonal (*VH* and *HV*) polarizations.

The development and use of polarimetric methods for studying land covers at present is associated with designing various decompositions of the complex polarization scattering matrix (Cloude, Pottier, 1996; Freeman, Durden, 1998; Yamaguchi et al., 2005; Minh et al., 2015). These decompositions allow us to obtain polarization «portraits» of the sensed objects and identify physical mechanisms of radar backscattering. It makes possible then to perform an accurate radar sensing data interpretation. One of the famous methods of polarization analysis is a graphical representation of the backscatter coefficient for all possible states of the polarization ellipse, which is realized in the form of a polarization signature (van Zyl et al., 1987). Recently, there has been newly proposed polarization signatures, in which a parameter under investigation is a coherence (Jafari et al., 2015). As shown in (Strzelczyk, Porzycka-Strzelczyk, 2014) the polarization signatures can identify coherent scatterers. In (De Grandi et al., 2003) the polarimetric texture signature has been introduced for the analysis of polarimetric radar images. It shows in graphical form the dependency of the normalized second-order moment of intensity on polarization state. The second moment of backscattered power characterizes statistically the variation of the radar signal due to speckle and the underlying radar cross section.

Along with the development of polarimetric radar techniques, there are articles where texture analysis methods are used, including fractal approach. In (Riccio, Ruello, 2015) it is pointed out that fractal models improved the interpretation of remote-sensing products due to their universally recognized ability to characterize natural surfaces, their interaction with electromagnetic fields and the corresponding (both multispectral and radar) images. Reference (Di Martino et al., 2014) shows that the fractal dimension maps can provide an anisotropy indication of the fractal characteristics of an observed surface. Moreover, the SAR image fractal dimension can be a feature that provides a measure of the image roughness (Berizzi et al., 2006). So we may assume that a given image roughness will show the degree of volume heterogeneity of targets, forests especially. The trunks and large branches of trees are discrete strong scatterers (Dobson et al., 1992). They all have different angles of inclination and represent the three-dimensional architecture of the forest. Therefore, it makes sense to estimate the fractal dimension not only for horizontal or vertical polarizations but also for different shapes of polarization ellipse.

The paper proposes a new approach for estimating of volume target heterogeneity, which is based on a fractal analysis of the PolSAR data. We propose to calculate the fractal dimension (FD) for a small fragment of a radar image for all possible states of polarization ellipse. Thus, we get multi-fractal dimension of that fragment which characterize the degree of radar backscattering heterogeneity at various angles of orientation and ellipticity. A graphical representation of this multi-fractal dimension will represent a polarization signature of spatial variations of the radar backscattering. Such fractal polarization signature may characterize, for example, the angular distribution of the trees branches in a vertical plane, or the azimuthal distribution of the branches when imaging from ascending and descending orbits. Until recently, the fractal approach has been used in cases of linear polarization for the analysis of the inhomogeneous medium in the form of the forest (Chimitdorzhiev, Dmitriev, 2009).

THEORY

The core of the proposed method is the application of fractal image analysis in process of polarization signatures generation.

Polarization signature. The significant advantage of multi-polarization radar is realized in it possibility to synthesize polarization response of a scatterer for any desired combination of transmit and receive antenna polarizations even they were not recorded by the radar.

The most general relationship between the incident and received fields may be expressed in the form of a matrix equation (Richards, 2009):

$$\begin{bmatrix} E_H^r \\ E_V^r \end{bmatrix} = \frac{e^{ikd}}{d} \begin{bmatrix} S_{HH} & S_{HV} \\ S_{VH} & S_{VV} \end{bmatrix} \begin{bmatrix} E_H^i \\ E_V^i \end{bmatrix}$$

or,

$$E^r = \frac{e^{ikd}}{d} SE^i. \qquad (1)$$

Here E^r and E^i are the vectors of received and incident field respectively, S is referred to as the scattering matrix or Sinclair matrix of the scatterer, d is a wave propagation path, k is a phase constant. It should be pointed out that subscripts H and V of matrix elements mean horizontal (H) and vertical (V) polarizations. The first subscript on each of the elements refers to the polarization of the scattered wave while the second subscript refers to the polarization of the incident wave.

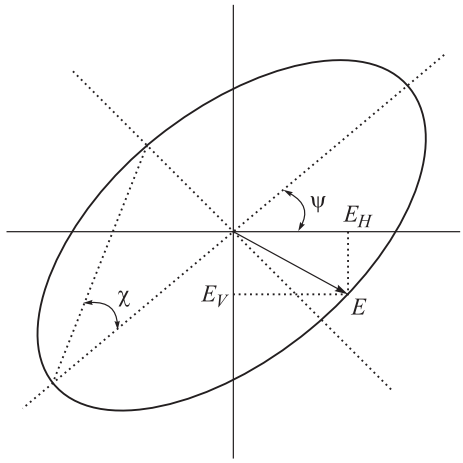

Fig. 1. Polarization ellipse.

It is known that polarization state of the electromagnetic wave can be represented in the shape of polarization ellipse. Such ellipse is completely described by two geometrical parameters, the ellipse orientation angle y and the ellipticity angle χ (Fig. 1).

The handedness of the polarization is indicated by the sign of ellipticity angle. Note that the range of χ is –45° to +45° and the range of ψ is 0° to 180°.

In the radar technique the power density relationships in an electromagnetic wave is very convenient to describe by means of Stokes parameters. In terms of ellipse orientation angle ψ and the ellipticity angle χ they are defined in normalized form by

$$s_0^2 = s_1^2 + s_2^2 + s_3^2,$$
$$s_1 = \cos 2\psi \cos 2\chi,$$
$$s_2 = \sin 2\psi \cos 2\chi,$$
$$s_3 = \sin 2\chi.$$

Often Stokes parameters are collected together into a column vector called Stokes vector $s = [s_0\ s_1\ s_2\ s_3]^T$, were superscript T means vector transpose operation.

As for field vectors in (1) there is an equation that relates Stokes vector of the received wave s^r to the Stokes vector of incident wave s^i:

$$s^r = \frac{1}{d^2} RR^T M s^i.$$

The real 4 × 4 matrix M is called the Stokes scattering operator or Stokes matrix. Its elements are the functions of the scattering matrix S and can be expressed as:

$$M = (R^{-1})^T W R^{-1},$$

where

$$W = \begin{bmatrix} S_{HH}S_{HH}^* & S_{HV}S_{HV}^* & S_{HH}S_{HV}^* & S_{HV}S_{HH}^* \\ S_{VH}S_{VH}^* & S_{VV}S_{VV}^* & S_{VH}S_{VV}^* & S_{VV}S_{VH}^* \\ S_{HH}S_{VH}^* & S_{HV}S_{VV}^* & S_{HH}S_{VV}^* & S_{HV}S_{VH}^* \\ S_{VH}S_{HH}^* & S_{VV}S_{HV}^* & S_{VH}S_{HV}^* & S_{VV}S_{HH}^* \end{bmatrix},$$

$$R = \begin{bmatrix} 1 & 1 & 0 & 0 \\ 1 & -1 & 0 & 0 \\ 0 & 0 & 1 & 1 \\ 0 & 0 & -i & i \end{bmatrix}.$$

The asterisk sign denotes complex conjugation.

The knowledge of the Stokes matrix permits synthesis of the radar cross section s of a scatterer for any transmit and receive polarization combination:

$$\sigma(\psi^r, \chi^r, \psi^t, \chi^t) = 4\pi (s^r)^T M s^t, \qquad (2)$$

where

$$(s^r)^T = [1\ \ \cos 2\psi^r \cos 2\chi^r\ \ \sin 2\psi^r \cos 2\chi^r\ \ \sin 2\chi^r],$$
$$s^t = [1\ \ \cos 2\psi^t \cos 2\chi^t\ \ \sin 2\psi^t \cos 2\chi^t\ \ \sin 2\chi^t]^T$$

and ψ^r and χ^r are the ellipse orientation angle and ellipticity angle of the received wave respectively, whereas ψ^t and χ^t are the same angles of the transmitted wave.

The function $\sigma(\psi^r, \chi^r, \psi^t, \chi^t)$ as described by (2) is called polarization signature (van Zyl et al., 1987) of the scatterer. Since the polarization signature is a function of four quantities, representation of the most general signature is awkward. Conventionally, the case where transmit and receive polarizations are identical is used (i. e. $\psi^r = \psi^t$, $\chi^t = \chi^t$). Such signature is referred to as co-polarized signature. Alternatively, if the receiver polarization is orthogonal to the transmitter polarization the resulting signature is referred to as cross-polarized. For this case:

$$\psi^r = \psi^t + 90°,\ \ \chi^r = -\chi^t.$$

Fractal analysis. Estimating fractal dimensions (FD) is the principal way of quantitatively describing the fractal properties or nonhomogeneous of the three-dimensional spatial objects being studied. Until recently, Mandelbrot's and van Ness' fractional Brownian motion (fBm) probably provides the most useful mathematical model for the random fractals found in nature (Chen et al., 1989; Xu et al., 1993; Addison, Ndumu, 1999). In order to apply the fBm to the original radar image, it is considered as a three-dimensional spatial surface with (x, y) denoting pixel position on the image plane, and the

third coordinate $z = I(x, y)$ denoting the value of radar backscattering. This surface must satisfy the following relationship in the fBm model (Xu et al., 1993):

$$E(|I(x_2, y_2) - I(x_1, y_1)|) \propto \propto \left(\sqrt{(x_2 - x_1)^2 + (y_2 - y_1)^2}\right)^H, \quad (3)$$

where $E(...)$ denotes expectation value, and H is called the Hurst index ($0 < H < 1$). This fBm surface is enveloped in three-dimensional space and has the following major properties:

1) the surface is continuous, but non-differentiable, and every property of this surface is dependent on the single scaling parameter H;

2) the fractal dimension of the surface is $D = 3 - H$;

3) the surface is self-affine.

Equation (3) can be rewritten as $E(\Delta I_{\Delta r}) = K\Delta r^H$, where $\Delta I_{\Delta r} = |I(x_2, y_2) - I(x_1, y_1)|$, $\Delta r = \sqrt{(x_2 - x_1)^2 + (y_2 - y_1)^2}$, and K is a constant. By applying the log function to both of the equation, we obtain

$$\log(E(\Delta I_{\Delta r})) = H \log(\Delta r) + \text{constant}. \quad (4)$$

Equation (4) is used for the estimation of fractal dimension of an image surface in the following manner. First, we calculate the quantity of $E(\Delta I_{\Delta r})$ for various Δr. Second, we take log of $E(\Delta I_{\Delta r})$ and Δr, and plot the $\log(E(\Delta I_{\Delta r}))$ versus $\log(\Delta r)$. Then, a least-square linear regression is used to estimate the slope of the resultant curve, which will be the H value. From H we can obtain the fractal dimension, $D = 3 - H$. Complete description of the process of fractal dimension estimation has been presented in (Chen et al., 1989).

Fractal polarization signature. The flowchart of the algorithm for constructing the fractal polarization signature is shown in Fig. 2.

At the first step, the ranges of variation of the orientation angle ψ and ellipticity angle χ of the polarization ellipse are divided into uniform sequences of the values $\psi_i = \psi_{i-1} + \Delta\psi$ ($i = 0, 1, \ldots, N$; $\psi_0 = 0°$; $\psi_N = 180°$) and $\chi_j = \chi_{j-1} + \Delta\chi$ ($j = 0, 1, \ldots, M$; $\chi_0 = -45°$; $\chi_M = +45°$). For each combination (ψ_i, χ_j) a co-polarized or cross-polarized image is synthesized in accordance with (2). Then the synthesized images are transformed into fractal images. A fractal image is obtained by calculating the FD of each pixel over the whole synthesized image. The FD value of each pixel is obtained by calculating the fractal dimension of a 7 × 7 pixel block centered on this pixel (Chen et al., 1989). A software that implements fractal image creation described in (Tustison, Gee, 2009). A region of interest (ROI) for which the signature has to be constructed is defined in these images. The calculated FDs in the chosen ROI are averaged for obtaining the resultant FD. Thus, one value of D_{ij} is obtained for each pair of the angles (ψ_i, χ_j). The resultant set of $L = (N + 1) \times (M + 1)$ points (ψ_i, χ_j, D_{ij}) forms the FPS, which characterizes the spatial fluctuations of the radar backscattering.

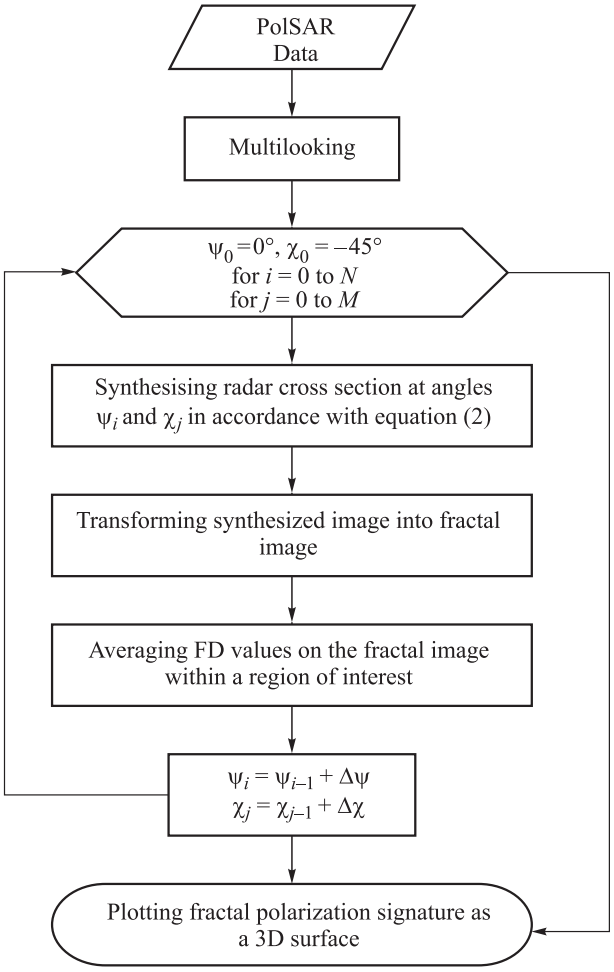

Fig. 2. The flowchart of fractal polarization signature generation. $\Delta\psi$ and $\Delta\chi$ are the increment steps of appropriate angles.

The software developed by the authors was used for FPS calculation. It is based on Orfeo ToolBox an open-source project for state-of-the-art remote sensing (Orfeo, 2016). The software is written on C++ programming language and contains several additional utilities for radar data preprocessing beside the main application for signatures calculation. The source code is available on GitHub (Fractal…, 2017).

It should be noted that FPS construction is computationally expensive. The reason is that estima-

tion of the value of one pixel of the fractal image requires processing of $s \times s$ pixels of the original image, where s is a pixel block size. Thus, the number of computations for determining only one FD value increases as a square of the block size. Another factor affecting the computation time is the choice of the step of variation of the polarization ellipse angles. Let $\Delta\psi = \Delta\chi = \delta$ be the step of the sequences of variation of the polarization ellipse angles. Then we have $N = \lfloor 180° / \delta \rfloor$ and $M = \lfloor 90° / \delta \rfloor$. For $\delta = 3°$, we obtain $N = 60$ and $M = 30$. For FPS construction, it is necessary to synthesize $L = 1891$ polarimetric images and to transform each image to a fractal image. Depending on the original radar image size, it takes several hours on a personal computer (64-bit computer with an Intel® Core™ i5-2310@2.9 GHz processor). For a step of 1°, it is necessary to process $L = 16\,471$ images, which substantially increases the computation time.

DATASET DESCRIPTION

Fig. 3 shows the Google Maps image of the area being studied.

It is located approximately in 75 km northwest from Ulan-Ude, Russia near the eastern coast of the Baikal Lake. The study area was a flat region with size approximately equaled 2.5 km^2 consisting mostly from pine forest *Pinus sylvestris*. The inventory description of the forest was collected from the forestry maps and field surveys. They showed that average trees density varies from 0.1 to 0.25 tree/m^2, whereas diameter of stems is in the range from 0.15 to 0.28 m. Azimuthal distribution of trees branches was measured in several sub areas within the study area. These measurements have ascertained that more than fifty percent of trees have the greater number of branches in the range of the azimuthal angles from south-east to the south-west (Fig. 4.).

Fig. 5 depicts the typical forest stand with trees branches oriented mostly in south-southeast direction.

For constructing the signatures, we used the data of spaceborne polarimetric SAR: SIR-C, which made imaging in October 1994, and ALOS, which made imaging in 2006–2009 (see Table).

SIR-C images were simultaneously obtained in two frequency ranges: L- and C-bands with wave-

Fig. 3. Test area on the Google Maps and geometry of radar imaging for SIR-C (arrow 1) and ALOS PALSAR at ascending (arrow 2) and descending (arrow 3) orbits.

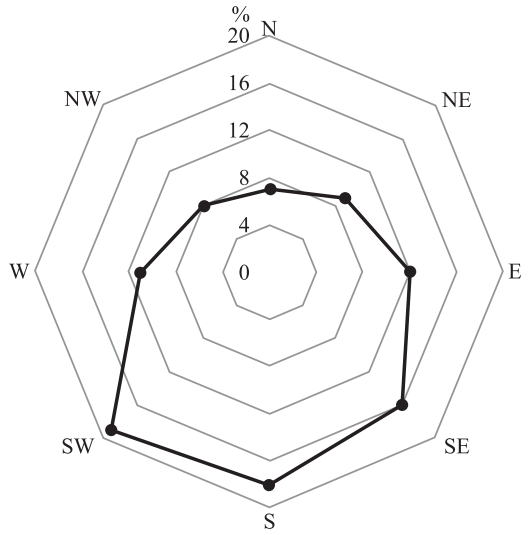

Fig. 4. Azimuth distribution of the trees' branches. The strength in each direction is the frequency of branch azimuths.

Fig. 5. A typical forest stand in the study area.

lengths of 24 and 5.6 cm, respectively. Imaging was performed at the ascending orbit towards the south-southeast (see arrow 1 in Fig. 3) due to the fact that orbit inclination angle is equal to 62.6 degrees.

The angle of inclination of the ALOS PALSAR orbit equaled 98.1 degrees, and when the sensing was performed at the ascending orbit, it was close to the east (arrow 2).

Also, the direction of sensing was moved to the west (arrow 3), at the descending orbit. Multilooking was performed for the initial data in order to eliminate the speckle noise. As a result, the size of the pixel in the images equaled 24 × 24 m.

Polarimetric radar data

SAR system	Orbit inclination angle	Acquisition dates
SIR-C	62.6°	09.10.1994 10.10.1994
ALOS PALSAR, ascending orbit	98.1°	28.06.2006 13.08.2006 28.09.2006 13.11.2006 31.03.2007 16.05.2007 16.11.2007 02.04.2008 05.04.2009
ALOS PALSAR, descending orbit	98.1°	30.05.2006 15.07.2006 30.08.2006 15.10.2006

RESULTS AND DISCUSSION

Fig. 6 shows three different types of co-polarized signatures which were calculated for the study area.

These are classic (van Zyl et al., 1987), second moment, and fractal signatures. The signatures were computed for all available data (see Table) and then averaged depending on the direction of the satellites orbit. The second moment signature was calculated as classic polarization signature except plotting standard deviation of radar cross section values in the area being studied instead of their average value.

The abscissa axis on Fig. 6 shows the ellipse orientation angle ψ, the ordinate axis shows the ellipticity angle χ. Along the *z*-axis the normalized radar cross section s is presented on Fig. 6, *a*, *b*, *c*, standard deviation on Fig. 6, *d*, *e*, *f*, and fractal dimension *D* on Fig. 6, *g*, *h*, *i*. Consider dependencies on the orientation angle, assuming that the dependence of the ellipticity angle is symmetrical relative to the linear polarization. The fractal signatures shown in Fig. 6, *g* also have a symmetrical distribution with respect to the orientation angle of 90°, which corresponds to the vertical polarization.

The values of the FD greater than 2.85, correspond to significant spatial variations of the radar backscattering (Chimitdorzhiev, Dmitriev, 2009). However, these variations correlate with the spatial distribution of inhomogeneities such as tree trunks and large tree branches. A certain symmetry (Fig. 6, *g*) of the signature with respect to the ellipse orientation angle being equal to 90º (vertical polarization), is associated with the similar distribution of

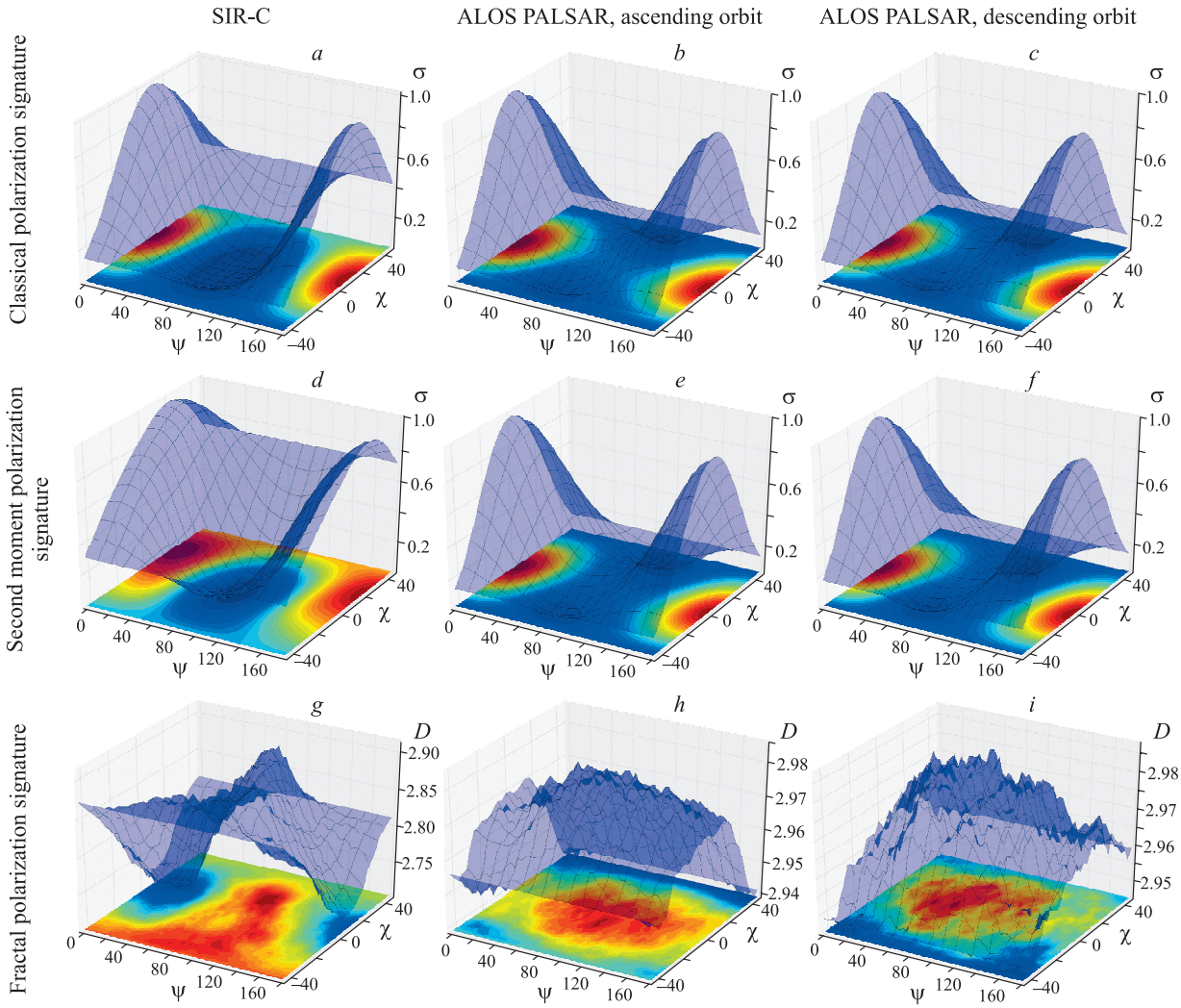

Fig. 6. Classic, second moment, and fractal co-polarized signatures estimated from the data of SIR-C (*a*, *d*, *g*), and ALOS PALSAR at ascending (*b*, *e*, *h*) and descending (*c*, *f*, *i*) orbits.

branches from the western and eastern sides of the trees when sensing to the south (in case of SIR-C).

By ALOS PALSAR sensing at the ascending orbit (Fig. 6, *h*), i. e., towards the east, there is a marked distribution of spatial variations (the FD being more than 2.97) in the range of orientation angles equal to 90°–170°.

With this geometry sensing (see Fig. 3), whenever the zero orientation angle coincides with the direction towards the south, a similar angular distribution testifies that tree branches form a denser reflection layer from the south, and the branches are less dense from the north, respectively. Conversely, at descending orbits, and sensing towards the west (so the zero orientation angle coincides with the north), there is an increasing number of spatial variations observed when orientation angles ranged from 20 to 90 degrees (Fig. 6, *i*). This may also be due to the higher density of branches, growing to the south.

Compare the obtained results with the help of one of the well-known method for evaluating the state of polarization on the example of ALOS PALSAR data. Let us consider histograms of the Stokes parameter s_2 computed from the images of the area being studied (Fig. 7).

The Stokes parameter s_2 estimates the relationship between linearly polarized components of electromagnetic wave with $\psi = +45°$ and $\psi = -45°$. There are three cases for the values of s_2:

1) $s_2 > 0$, then ψ is tend to be +45°;
2) $s_2 < 0$, then ψ is tend to be –45°;
3) $s_2 = 0$, then ψ has no predominant value.

The Stokes parameter was calculated by PolSARpro software (version 5.0.4) (PolSARpro, 2015) with window size being equal 5 × 5 pixels. The histogram for the ascending orbit shows a slight predominance of positive values of the s_2 parameter.

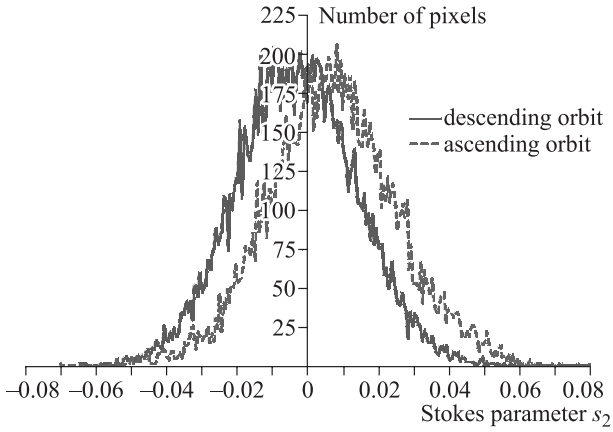

Fig. 7. The histogram of the Stokes parameter s_2 distribution in the study area.

When we consider images taken from ascending orbit (see Fig. 3, arrow 2) this may indicate more depolarization and a larger number of elementary scatterers located at an angle of 45° on the south side of the trees. The prevalence of negative values in the histogram for the descending orbit is an indicator of the dominance of the radar backscattering with angle equal to –45°. However, the sensing was carried out in the opposite direction (see Fig. 3, arrow 3), so we can conclude about the presence of a larger number of scatterers at an angle of 45 degrees in a southerly direction. This confirms the results obtained by analyzing fractal polarization signature.

CONCLUSION

The paper proposes novel approach for analysis of full polarimetric SAR images. This approach based on new type of polarization signatures for assessing the structure of the spatial variations of radar backscattering. In order to plot the signature, we used fractal analysis, which assumes self-similarity of the objects being studied at different spatial scales. The proposed fractal signature allows us to estimate the anisotropy of the spatial distribution of discrete inhomogeneities, for example, the branches of the trees. The azimuthal dependence in intensity distribution of the radar backscattering is found when analyzing the radar remote sensing data of a pine forest. It correlates with the results of a field survey of the trees branches distribution.

This work was supported in part by the Federal agency of scientific organizations and Russian Foundation for Basic Research (Grant No. 16-08-00646 A). Original ALOS PALSAR data granted by Japan Aerospace Exploration Agency (JAXA) under ALOS-2 RA-6 (PI number: 3092).

REFERENCES

Addison P. S., Ndumu A. S. Engineering applications of fractional Brownian motion: self-affine and self-similar random processes // Fractals. 1999. V. 7. N. 02. P. 151–157.

Berizzi F., Bertini G., Martorella M., Bertacca M. Two-dimensional variation algorithm for fractal analysis of sea SAR images // IEEE Trans. Geosci. Rem. Sens. 2006. V. 44. N. 9. P. 2361–2373.

Chen C.-C., DaPonte J. S., Fox M. D. Fractal feature analysis and classification in medical imaging // IEEE Trans. on Medical Imaging. 1989. V. 8. N. 2. P. 133–142.

Chimitdorzhiev T. N., Dmitriev A. V. Processing and interpretation methodology of radar images by multifractal analysis // Vychislitel'nye Tekhnologii (Computational Technologies). 2009. V. 14. N. 1. P. 116–124 (in Russian with English abstract).

Cloude S. R., Pottier E. A review of target decomposition theorems in radar polarimetry // IEEE Trans. Geosci. Rem. Sens. 1996. V. 34. N. 2. P. 498–518.

De Grandi G., Lee J.-S., Schuler D., Nezry E. Texture and speckle statistics in polarimetric SAR synthesized images // IEEE Trans. Geosci. Rem. Sens. 2003. V. 41. N. 9. P. 2070–2088.

Di Martino G., Franceschetti G., Iodice A., Riccio D., Ruello G., Zinno I. Fractal dimension estimation from fully polarimetric SAR data // Proc. IGARSS-2014. P. 3482–3485.

Dobson M. C., Ulaby F. T., LeToan T., Beaudoin A., Kasischke E. S., Christensen N. Dependence of radar backscatter on coniferous forest biomass // IEEE Trans. Geosci. Rem. Sens. 1992. V. 30. N. 2. P. 412–415.

Fractal Polarization Signature (Source Code). 2017. https://github.com/AlekseyDmitriev/fractal-polarization-signature.git

Freeman A., Durden S. L. A three-component model for polarimetric SAR imagery // IEEE Trans. Geosci. Rem. Sens. 1998. V. 36. N. 3. P. 963–973.

Jafari M., Maghsoudi Y., Zoej M. A new method for land cover characterization and classification of polarimetric SAR data using polarimetric signatures // IEEE J. Sel. Topics Appl. Earth Observ. Rem. Sens. 2015. V. 99. P. 1–13.

Minh N., Zou B., Zhang Y., Le V. General three-layer scattering model for forest parameter estimation using single-baseline polarimetric interferometry synthetic aperture radar data // J. Appl. Rem. Sens. 2015. V. 9. N. 1. P. 096043.

Orfeo ToolBox Project. 2016. https://www.orfeo-toolbox.org/

PolSARpro Software. Version 5.0.4. 2015. https://earth.esa.int/web/polsarpro

Riccio D., Ruello G. Synthesis of fractal surfaces for remote-sensing applications // IEEE Trans. Geosci. Rem. Sens. 2015. V. 53. N. 7. P. 3803–3814.

Richards J. A. Remote sensing with imaging radar. Berlin; Heidelberg: Springer-Verlag, 2009. 361 p.

Sinha S., Jeganathan C., Sharma L. K., Nathawat M. S. A review of radar remote sensing for biomass estimation // Int. J. Environ. Sci. Technol. 2015. V. 12. N. 5. P. 1779–1792.

Strzelczyk J., Porzycka-Strzelczyk S. Identification of coherent scatterers in SAR images based on the analysis of polarimetric signatures // IEEE Geosci. Rem. Sens. Letters. 2014. V. 11. N. 4. P. 783–787.

Tustison N., Gee J. Stochastic fractal dimension image // The Insight J. 2009. http://hdl.handle.net/1926/1525

van Zyl J. J., Zebker H. A., Elachi C. Imaging radar polarization signatures: theory and observation // Radio Sci. 1987. V. 22. N. 4. P. 529–534.

Xiao Rui, Meng Li, Fengri Li. Branching structure analysis of Scotch pine plantation // World Rural Observ. 2015. V. 7. N. 1. P. 26–31. http://www.sciencepub.net/rural/rural070115/004_A00363rural070115_26_31.pdf

Xu T., Moore I. D., Gallant J. C. Fractals, fractal dimensions and landscapes – a review // Geomorphology. 1993. V. 8. N. 4. P. 245–262.

Yamaguchi Y., Moriyama T., Ishido M., Yamada H. Four-component scattering model for polarimetric SAR image decomposition // IEEE Trans. Geosci. Rem. Sens. 2005. V. 43. N. 8. P. 1699–1706.

УДК 528.87 + 528.855

АНАЛИЗ ПРОСТРАНСТВЕННЫХ ВАРИАЦИЙ ПОЛЯРИМЕТРИЧЕСКОГО ОБРАТНОГО РАДАРНОГО РАССЕЯНИЯ ДЛЯ ОЦЕНКИ АНИЗОТРОПИИ ЛЕСА

А. В. Дмитриев, Т. Н. Чимитдоржиев, П. Н. Дагуров

Институт физического материаловедения СО РАН
670047, Республика Бурятия, Улан-Удэ, ул. Сахьяновой, 6

E-mail: scidir@ipms.bscnet.ru

Поступила в редакцию 01.12.2016 г.

Предлагается новый метод дистанционной оценки пространственной неоднородности лесной среды на основе данных поляриметрических радиолокаторов космического базирования (PolSAR). Существенным преимуществом поляриметрических радиолокаторов является их возможность синтезировать поляризационный отклик при любой ориентации передающей и приемной антенн. Это позволяет лучше выявлять доминирующие механизмы рассеяния, особенно при анализе поляризационных сигнатур. Такие сигнатуры дают более детальную физическую информацию об обратном рассеянии в различных поляризационных базисах. Однако поляризационные сигнатуры не могут выявить пространственные вариации обратного рассеяния, вызванные объемной неоднородностью объекта исследования (например, ветвями деревьев в лесу). Поэтому предлагается новый подход для оценки объемной неоднородности рассеивателей, использующий поляриметрические изображения радиолокаторов с синтезированной апертурой. Предложенный метод основан на анализе нового типа поляризационной сигнатуры – фрактальной поляризационной (ФПС). Такая сигнатура представляется в виде трехмерного графика и может быть построена для каждого пикселя исходного изображения. Показано, что ФПС описывает вариации обратного рассеяния (или вариации яркости пикселей изображения) при различных состояниях поляризации. Для тестирования метода использованы полностью поляриметрические изображения космических радиолокаторов SIR-C и ALOS PALSAR на восходящих и нисходящих орбитах. При анализе обратного рассеяния от соснового леса обнаружена азимутальная зависимость пространственных вариаций радарного рассеяния. Данная зависимость коррелирует с результатами полевого исследования, показывающими некоторое преобладание количества ветвей деревьев с южной стороны соснового леса.

Ключевые слова: *радарная съемка, поляризационная сигнатура, фрактальная размерность, пространственные вариации*.